A PAS Domain with an Oxygen Labile [4Fe-4S]$^{2+}$ Cluster in the Oxygen Sensor Kinase NreB of *Staphylococcus carnosus*[†]

Martin Müllner,[‡] Oliver Hammel,[‡] Bernd Mienert,[§] Steffen Schlag,[||] Eckhard Bill,[§] and Gottfried Unden*[,‡]

Institut für Mikrobiologie and Weinforschung, Universität Mainz, Becherweg 15, 55099 Mainz, Germany, Max-Planck Institut für Bioanorganische Chemie, Stiftsstrasse 34−36, 45470 Mülheim, Germany, and Mikrobielle Genetik, Universität Tübingen, 72076 Tübingen, Germany

Received July 28, 2008; Revised Manuscript Received October 17, 2008

ABSTRACT: The cytoplasmic histidine sensor kinase NreB of *Staphylococcus carnosus* responds to O_2 and controls together with the response regulator NreC the expression of genes of nitrate/nitrite respiration. *nreBC* homologous genes were found in *Staphylococcus* strains and *Bacillus clausii*, and a modified form was found in some *Lactobacillus* strains. NreB contains a sensory domain with similarity to heme B binding PAS domains. Anaerobically prepared NreB of *S. carnosus* exhibited a (diamagnetic) [4Fe-4S]$^{2+}$ cluster when assessed by Mössbauer spectroscopy. Upon reaction with air, the cluster was degraded with a half-life of ~2.5 min. No significant amounts of Mössbauer or EPR detectable intermediates were found during the decay, but magnetic Mössbauer spectra revealed formation of diamagnetic [2Fe-2S]$^{2+}$ clusters. After extended exposure to air, NreB was devoid of a FeS cluster. Photoreduction with deazaflavin produced small amounts of [4Fe-4S]$^{+}$, which were degraded subsequently. The magnetically perturbed Mössbauer spectrum of the [4Fe-4S]$^{2+}$ cluster corroborated the $S = 0$ spin state and revealed uniform electric field gradient tensors of the iron sites, suggesting full delocalization of the valence electrons and binding of each of the Fe ions by four S ligands, including the ligand to the protein. Mutation of each of the four Cys residues inactivated NreB function in vivo in accordance with their role as ligands. [4Fe-4S]$^{2+}$ cluster-containing NreB had high kinase activity. Exposure to air decreased the kinase activity and content of the [4Fe-4S]$^{2+}$ cluster with similar half-lives. We conclude that the sensory domain of NreB represents a new type of PAS domain containing a [4Fe-4S]$^{2+}$ cluster for sensing and function.

Adaptation of the metabolism and cell composition to the availability of oxygen is significant for many bacteria that are not restricted permanently to aerobic and anaerobic metabolism (*1, 2*). By using oxygen sensors, the bacteria are able to control the expression of genes for enzymes and pathways which are required for either aerobic, microaerobic, or anaerobic metabolism, and the synthesis of protective enzymes. A remarkable range of oxygen sensors has been described, which are able to use diverse devices for sensing oxygen, either by direct reaction with molecular oxygen (FeS, heme B, and Cys thiols) or by interaction with a metabolite responding to the presence of oxygen in energy metabolism (e.g., NADH/NAD or QH_2/Q ratios) (*3, 4*).

FNR[1] (fumarate nitrate reductase regulator) of *Escherichia coli* is one of the best-characterized bacterial oxygen sensors (*3−6*). FNR is a transcriptional regulator of the CRP/FNR family with a helix−turn−helix domain for DNA binding. In the active (anaerobic) state, FNR is a dimer, and each of the monomers hosts a [4Fe-4S]$^{2+}$ cluster which is liganded by four cysteine residues (*7−9*). The FNR dimer binds to promoters of target genes and controls the binding and function of RNA polymerase. Even at low concentrations in the medium, O_2 diffuses into the cytoplasm of the bacteria where it directly reacts with FNR (*10, 11*). After an initial oxidation of the [4Fe-4S]$^{2+}$ cluster and loss of one Fe^{2+}, FNR with a [2Fe-2S]$^{2+}$ cluster is formed which differs (formally) by the loss of two Fe^{2+} and two S^{2-} ions from the [4Fe-4S]$^{2+}$ cluster (*7, 12, 13*). FNR with the [2Fe-2S]$^{2+}$ cluster is monomeric and no longer active in gene regulation (*8*). Subsequently, the [2Fe-2S]$^{2+}$ cluster degrades, and cofactor-free apoFNR is formed which is the actual form of FNR in aerobically growing bacteria (*14, 15*). FNR_{Bs} from *Bacillus subtilis* is also a member of the CRP/FNR family of transcriptional regulators and uses a [4Fe-4S]$^{2+}$ cluster for O_2 sensing and control of function (*16, 17*). In FNR_{Bs}, binding of the FeS cluster differs from that in FNR of *E. coli*. In FNR, four Cys residues ligate the FeS cluster, three of which are at the N-terminal end of the protein (*3, 6*). The FeS cluster of FNR_{Bs} is bound by three Cys residues close to the C-terminal end of the protein, and one further unknown ligand.

Recently, the NreBC two-component system has been identified in the nonsporulating Gram-positive *Staphylococ-*

[†] The work was supported by grants from Deutsche Forschungsgemeinschaft to G.U. and the LGFG (Landesgraduierten Förderungsgesetz) to M.M.

* To whom correspondence should be addressed: Universität Mainz, Institut für Mikrobiologie and Weinforschung, Becherweg 15, 55099 Mainz, Germany. Telephone: +49-6131-3923550. Fax: +49-6131-3922695. E-mail: unden@uni-mainz.de.

[‡] Universität Mainz.

[§] Max-Planck Institut für Bioanorganische Chemie.

[||] Universität Tübingen.

[1] Abbreviations: CRP, cyclic AMP receptor protein; DTT, dithiothreitol; FNR, fumarate nitrate reductase regulator; NreB, nitrogen regulation.

10.1021/bi8014086 CCC: $40.75
Published on Web 12/04/2008

Table 1: Strains of *S. carnosus* and *E. coli* and Plasmids

	genotype or characteristics	ref
strains		
S. carnosus TM300	wild-type strain	*24*
S. carnosus m1	Δ*nreABC*::*ermB*	*18*
E. coli BL21(DE3) (pNifS)	*nifS* (*Azotobacter vinelandii*) expression strain	see ref *19*
E. coli JM109	*recA1 supE44 endA1 hsdR17 gyrA96 relA1 thi*(*lac-proAB*) F′[*traD36 proAB*$^+$, *lacI*^{q} *lacZM15*]	*44*
plasmids		
pCQE1	staphylococcal His-tag expression vector, xylose inducible, glucose repressible *xylA* promotor, *cam*^{R}	*18*
pRB473	*E. coli*/*S. carnosus* shuttle vector with *amp*^{R} for *E. coli* and *cam*^{R} *for S. carnosus*	*26*
pCQE1nreB	pCQE1 derivative carrying nreB on a *Hpa*I/*Bgl*II fragment	*18*
pRB473nreABC	pRB473 with *nreABC* and native promotor	this study
pRB473nreAB$_{C59A}$C	pRB473nreABC derivative with *nreB* encoding NreB-C59A	this study
pRB473nreAB$_{C62S}$C	pRB473nreABC derivative with *nreB* encoding NreB-C62S	this study
pRB473nreAB$_{C74S}$C	pRB473nreABC derivative with *nreB* encoding NreB-C74S	this study
pRB473nreAB$_{C77S}$C	pRB473nreABC derivative with *nreB* encoding NreB-C77S	this study

cus carnosus with low GC content (*18*). The NreBC (nitrogen regulation) system activates the expression of the *narGHJI*, *narT*, and *nirBD* genes encoding nitrate reductase, a putative nitrate/nitrite antiporter, and a cytoplasmic nitrite reductase, respectively, under anaerobic conditions. NreB is a cytoplasmic sensor kinase consisting of an N-terminal sensor and a C-terminal kinase domain. After treatment by procedures for in vitro insertion of FeS clusters, NreB exhibited spectral properties typical of FeS-containing proteins and increased kinase activity (*19*). The spectra were absent in NreB with a mutated Cys62 residue. The data suggest that NreB is a sensor using an FeS cluster for O_2 sensing; however, direct evidence for the presence of a FeS cluster was missing, and its type and role in controlling NreB function were not known.

The nature and role of the putative FeS cluster of NreB were studied in the isolated NreB protein and in vivo via mutation of the Cys residues representing the supposed ligands of the FeS cluster. The FeS cluster was identified by Mössbauer spectroscopy which represents the only means for identifying all types of FeS clusters, including diamagnetic or EPR-silent forms. It turned out that the sensory PAS domain contains an O_2-sensitive $[4Fe\text{-}4S]^{2+}$ cluster and represents a new type of PAS domain containing an FeS cluster. The presence of the cluster controls the kinase activity of the protein. The study shows that the PAS domain of NreB binds a $[4Fe\text{-}4S]^{2+}$ cluster which is rapidly destroyed by O_2, and the cluster destruction is related to the loss of kinase activity of NreB.

EXPERIMENTAL PROCEDURES

Growth and Bacteria. The bacterial strains used in this work are listed in Table 1. For isolation of anaerobic NreB, *S. carnosus* m1 (pCQE1nreB) which carried *nreB* on a plasmid under the control of an inducible *xylA* promotor (*20*) was grown in yeast extract production medium (YEPD) containing 45 g/L yeast extract (Servabacter 24540), 50 mM sodium phosphate (pH 7.2), 40 mM glycerol, 10 mM sodium nitrate, and 10 mM ferric ammonium acetate at 37 °C. The cells were grown under aerobic conditions on a rotary shaker (200 rpm) to an OD_{578} of 10−12, and then 150 mM xylose were added for 6 h. Afterward, the suspension was placed in 1 L bottles; the bottles were filled to the neck, sealed with stoppers, and incubated for 16 h at 4 °C (final OD_{578} of ∼50). For the enrichment of NreB·His with ^{57}Fe, all vessels for growing the bacteria were decontaminated with respect to natural Fe (*22*), and only analytical grade components with low Fe content and yeast extract were used. A $^{57}FeCl_3$ stock solution (179 mM) was prepared (*23*) and added to a final concentration of 80 μM instead of ferric ammonium acetate. *S. carnosus* strain m1 (pCQE1nreB) for aerobic preparation of NreB was grown as described previously (*19*).

For growth studies on the phenotype of NreB cysteine mutations, *S. carnosus* m1 (pRB473nreAB*C, where nreB* stands for variations in *nreB*), 5 mL of complex basic medium (BM) (*24*), and 1 mM nitrate were inoculated and incubated overnight under anaerobic conditions at 37 °C. For the growth experiment, 50 mL of BM medium with 1 mM nitrate was inoculated with 5 mL of the overnight culture in glass bottles (250 mL) with rubber stoppers. After the gas phase had been replaced with N_2 (99.99%), the bacteria were incubated on a rotary shaker at 160 rpm and 37 °C.

E. coli strains were grown in Luria-Bertani (LB) medium (10 g/L peptone, 5 g/L yeast extract, and 5 g/L NaCl) at 30 °C. Media were supplemented with ampicillin (100 μg/mL), chloramphenicol (10 μg/mL), or erythromycin (2.5 μg/mL) as appropriate. Aerobic cultures were incubated in Erlenmeyer flasks on a rotary shaker at 200 rpm. The flasks were filled to 16% of the maximal volume.

Preparation of Proteins. Aerobic NreB was prepared from *S. carnosus* strain m1 (pCQE1nreB) after growth and induction under aerobic conditions (*19*). Isolation of the protein was performed under air, but all buffers for protein preparation contained fresh β-mercaptoethanol (10 mM).

The procedure for preparation of anaerobic NreB was the same as for aerobic preparation, but all steps were performed under anoxic conditions. The preparation was performed in an anaerobic chamber (Coy) using anoxic buffers. For all other steps, the bacteria or solutions were filled in sealed containers before being handled outside the anaerobic chamber. The isolation procedure includes cell disruption in a cell mill, separation of the clear supernatant from debris by centrifugation, and chromatography on Ni-NTA-agarose (Qiagen). NreB-His_6 was eluted with buffer containing 300 mM NaCl, 20% (v/v) glycerol, 150 mM imidazole, and 50 mM sodium phosphate (pH 8). The samples eluting from the column and containing NreB were yellowish-brown in color. The sample (5−10 mL) was concentrated to 0.5 mL (20−25 mg of protein/mL) by solvent adsorption (Vivapore 10/20, MWCO 7.500, Sartorius VP-2003); 350 μL was transferred into a Mössbauer cuvette and frozen in liquid

N_2 which had been transferred in an open styrofoam box into the anaerobic chamber.

Cysteine desulfurase $NifS_{Av}$ from *Azotobacter vinelandii*, which is used for reconstituting the FeS cluster in NreB in vitro, was prepared from *E. coli* BL21(DE3)pNifS as described previously (*19*). The protein solution was stored at −80 °C, and each aliquot was frozen and thawed only once.

Reconstitution of Aerobic NreB. Reconstitution of the FeS cluster in aerobic NreB was performed with anoxic (degassed) buffers under an atmosphere of N_2 as described previously (*19*). Sulfide was prepared enzymatically by the addition of cysteine desulfurase $NifS_{Av}$, 1 mM cysteine, and 2.5 mM DTT. Fe was supplied as a solution of Mohr's salt, $(NH_4)_2[Fe(H_2O)_6](SO_4)_2$ (0.3−1.2 mM). For reconstitution with ^{57}Fe, the salt was prepared from metallic ^{57}Fe by being dissolved in 1 M H_2SO_4 at 110 °C under an atmosphere of N_2 and reflux conditions. The $^{57}FeSO_4 \cdot 7H_2O$ prepared in this way was converted to Mohr's salt by addition of a hot solution of $(NH_4)_2SO_4$ (aqueous). Mössbauer spectroscopy showed that the product obtained by the procedure was a mixture of 32% $(NH_4)_2[^{57}Fe(H_2O)_6](SO_4)_2$ and 68% $^{57}FeSO_4$. Aliquots of the salt were stored in the anaerobic chamber. Before use, 2 mg of the salt was dissolved in 50 μL of H_2O to produce a 100 mM stock solution. The reconstituted sample of NreB was desalted by gel filtration (Hitrap Desalting, GE Healthcare), transferred into Mössbauer cuvettes, and frozen in liquid N_2.

Oxidation, Reduction, and Air Exposure of NreB·[4Fe-4S]$^{2+}$. For reduction with dithionite, freshly prepared anaerobic NreB (0.25−0.5 mM) was incubated with an anoxic freshly prepared solution of sodium dithionite (final concentration of 5 mM, from a 50 mM stock) and incubated for up to 40 min. After UV−vis control, samples were placed into EPR tubes (180 μL) or Mössbauer cuvettes (350 μL), frozen in cold petrol ether and liquid nitrogen, and shipped at −80 °C for measurement. For photoreduction by deazaflavin (*25*), the anaerobic sample was first transferred to buffer containing 50 mM sodium phosphate, 300 mM NaCl, 20% (v/v) glycerol, 10 mM imidazole, and 20 mM sodium oxalate. The solution of NreB (300 μL, 0.4−0.9 mM) containing 41 μM deazaflavin was transferred into a rubber-stoppered quartz cuvette. The cuvette was illuminated at 4 °C by a slide projector (d = 30 cm). Every 10 min, the absorption spectrum of the sample was recorded. In control experiments, photoreduction was tested by the reduction of methylviologen added to the buffer. At specific time points, samples were withdrawn, frozen in cold petrol ether and liquid N_2, and shipped at −80 °C for EPR measurement. For exposure to air, anaerobic NreB (0.35−0.5 mL with 0.1−0.6 mM NreB) in buffer containing 50 mM sodium phosphate, 300 mM NaCl, 20% (v/v) glycerol, and 150 mM imidazole was transferred to a shallow polypropylene vessel (diameter of 4.5 cm) and shaken at room temperature under air. After specific time points, samples were withdrawn and frozen in Mössbauer cuvettes or EPR tubes in liquid N_2.

Autophosphorylation of NreB. Autophosphorylation of NreB was assessed with anaerobically prepared NreB under anoxic conditions in the anaerobic chamber. A solution of NreB in 7 μL (100−200 μM NreB) was diluted with 9 μL of reaction buffer [250 mM Hepes (pH 8.0), 250 mM KCl, 25 mM $MgCl_2$, 2.5 mM EDTA, 10 mM DTT, 26 μL of a buffer containing 50 mM sodium phosphate, 300 mM NaCl, 20% (v/v) glycerol, and 150 mM imidazole, and 2 μL of [^{33}P]ATP (0.22 μM with 5.5 TBq/mmol)]. Then, 30, 60, 90, 120, and 150 s after the reaction had been started by addition of [^{33}P]ATP, 4 μL samples were withdrawn and mixed with 8 μL of stop solution (SDS sample buffer) and subjected to SDS−PAGE on 12.5% polyacrylamide gels. After being wrapped in a transparent foil (Saran wrap), the gel was layered onto a Phosphor imaging plate (FUJIFILM BAS 2040 imaging plate) and exposed for 20−24 h at 4 °C. The plate was evaluated for radioactivity (or β-irradiation) in the FUJI BAS 1500 bioimaging analyzer, and relative contents of radioactivity were determined with Gel-Pro Analyzer 6.0 after the radioactivity of the complete bands had been counted and the background of the imager plate had been subtracted.

Genetic Methods. Plasmid pRB473nreABC was used for complementation of *S. carnosus* m1 (Δ*nreABC*::*ermB*). For construction, the 2.8 kb *nreABC* fragment was amplified by PCR using primers nreABC-*Bam*HI-F and nreABC-*Sal*I-R (Table 1 of the Supporting Information) from genomic DNA of *S. carnosus* TM300. The fragment comprises the complete *nreABC* operon, including the promoter and flanking *Bam*HI and *Sal*I sites. The fragment was cloned into the *Sal*I and *Bam*HI sites of plasmid pRB473 (*26*), resulting in pRB473*nreABC*. The Cys residues of NreB (Cys59, Cys62, Cys74, and Cys77) were replaced with Ser or Ala residues in plasmid pRB473nreABC by site-directed mutagenesis, using the QuickChange site-directed mutagenesis kit (Stratagene) and the primers given in Table 1 of the Supporting Information. The plasmids with the mutated *nreB* genes were amplified in *E. coli* JM109 and confirmed by sequencing of the *nreB* genes. The plasmid was isolated from *E. coli* and transformed into protoplasts of *S. carnosus* m1 (*24*). The medium for selection of transformants of *S. carnosus* contained chloramphenicol (10 μg/mL) and those of *E. coli* JM109 ampicillin (100 μg/mL).

Mössbauer and EPR Spectroscopy. Mössbauer spectra were recorded with alternating constant acceleration. The minimum experimental line width of the spectrometer was 0.24 mm s^{-1} (full width at half-height). The sample temperature was kept constant either in an Oxford Instruments Variox or in an Oxford Instruments Mössbauer-Spectromag cryostat. The latter is a split-pair superconducting magnet system for applied fields of up to 8 T, where the temperature of the sample can be varied in the range of 1.5−250 K. The field at the sample is perpendicular to the γ-beam. The ^{57}Co/Rh source (1.8 GBq) was positioned at room temperature inside the gap of the magnet system at a zero-field position. Isomer shifts are quoted relative to iron metal at 300 K.

X-Band EPR spectra were recorded on a Bruker ELEXSYS E500 spectrometer equipped with the Bruker standard cavity (ER4102ST) and a helium flow cryostat (Oxford Instruments ESR 910). Microwave frequencies were calibrated with a Hewlett-Packard frequency counter (HP5352B), and the field control was calibrated with a Bruker NMR field probe (ER035M). Spin quantification was accomplished by double integration of the experimental derivative spectra and comparison with a Cu(II) standard. Only linear corrections were invoked for adjustments of the experimental baseline.

Size-Exclusion Chromatography. A sample of 1.3 mL of anaerobic NreB (250 μM) was passed under anaerobic

conditions (anaerobic chamber) through a Superdex 200 prep grade HiLoad 16/60 column (GE Healthcare) at a flow rate of 1 mL/min. The column was equilibrated with a buffer containing 300 mM NaCl, 20% (v/v) glycerol, 150 mM imidazole, 5 mM DTT, and 50 mM sodium phosphate (pH 8). Protein content was monitored at 280 nm. Thyroglobulin (669 kDa), β-amylase (200 kDa), alcohol dehydrogenase (150 kDa), albumin (66 kDa), carbonic anhydrase (29 kDa), and cytochrome *c* (12.4 kDa) were used as standards. The anaerobic form of NreB was passed over the column directly after anaerobic preparation. To obtain the aerobic sample, the anaerobic sample (2 mL) was exposed to air for 40 min as described above, concentrated to a final volume of 1.3 mL, and passed over the Superdex 200 column in the same buffer as the anaerobic sample.

Analytical Methods. Nitrite was assessed colorimetrically (*27*) with sulfanilamide and *N*-(1-naphthyl)ethylenediamine, acid labile sulfide by the methylenblue method (*28*), and Fe ions with ferrocene after ashing of the samples (*29*) using standards for calibration. Protein was assessed with Roti-Quant (Carl Roth GmbH) and a solution of BSA for calibration. For Western blotting and immunoblotting, proteins were transferred by semidry blotting to nitrocellulose membranes and reacted with the primary antiserum (anti-penta His tag) and a secondary anti-rabbit antiserum which was coupled to horseradish peroxidase. Positive bands were detected by incubation with chloronaphthol.

RESULTS

A [4Fe-4S]$^{2+}$ Cluster in Anaerobically Prepared NreB. NreB was prepared under anoxic conditions from a *S. carnosus* NreB expression strain which was grown and induced under aerobic conditions to produce high cell yields and levels of expression. After induction and expression of high levels of NreB, the bacteria were incubated overnight under anaerobic conditions to convert NreB to the anaerobic form. From broken cells NreB was isolated under strict anoxic conditions, yielding 8.3 mg of purified NreB from 1 L of culture. The preparation of NreB differed from a previously described oxic preparation (*24*). The anaerobic protein solution was brownish in color and showed an absorption spectrum with shoulders at 325 and 420 nm (Figure 1). The color and absorption bands were lacking in NreB from aerobic bacteria, or after preparation of the protein in the presence of air (*19*). The shoulders at 325 and 425 nm (Figure 1) are characteristic of [4Fe-4S] cluster-containing proteins (*7, 9*).

The nature of the putative FeS cluster was studied by Mössbauer spectroscopy. The protein was labeled with ^{57}Fe that was added to the medium as the sole additional source of iron. Analysis of the iron content in the medium before and after the supply of ^{57}Fe showed that 78% of the iron was enriched, and the residual natural iron was introduced mainly by the yeast extract. The anoxic preparation of NreB had a Mössbauer spectrum which suggested the presence of two different forms of iron (Figure 2). The major component comprising 83% of the total iron of the anaerobic NreB exhibited a quadrupole doublet with an isomeric shift (δ = 0.44 mm/s) and a quadruple splitting (ΔE_Q = 1.16 mm/s) that are characteristic of [4Fe-4S]$^{2+}$ clusters of the ferredoxin type. The values are distinctly different from those expected

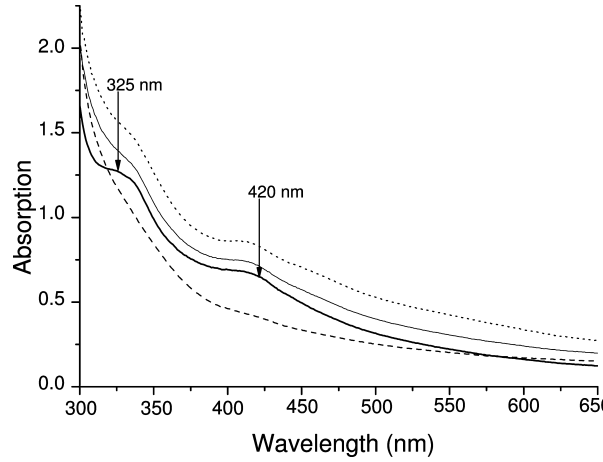

FIGURE 1: Effect of O_2 on the absorption spectrum of anoxically purified NreB of *S. carnosus*. Spectra of anoxically isolated NreB (0.25 mM) before (thick line) and after exposure for 1 (thin line) and 30 min (dotted line) to air. The spectrum of aerobically prepared NreB [0.4 mM (dashed line)] is shown for comparison.

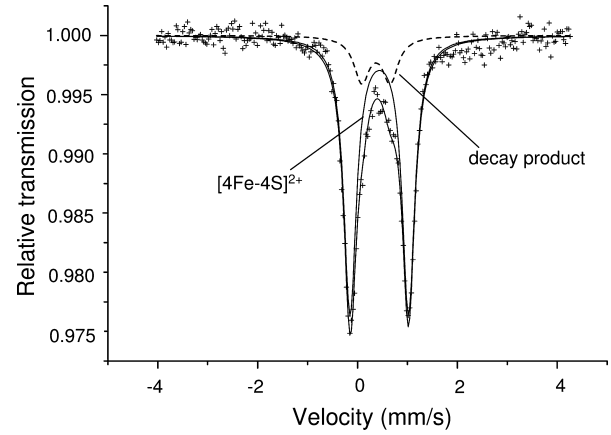

FIGURE 2: Zero-field Mössbauer spectrum of anaerobically isolated NreB (0.66 mM) recorded at 80 K. The solid line through experimental data is a superposition of two Lorentzian doublets with isomer shifts and quadrupole splittings (δ = 0.44 mm/s and ΔE_Q = 1.16 mm/s for the first doublet, and δ = 0.37 mm/s and ΔE_Q = 0.57 mm/s for the second doublet). The parameters for the first are typical of mixed-valent Fe(II)/Fe(III) as found in [4Fe-4S]$^{2+}$ clusters coordinated by four Cys residues.

for [2Fe-2S]$^{2+}$ or [3Fe-4S]$^{+}$ clusters. A minor component amounting to 17% of iron could be simulated with a second doublet showing a δ of 0.37 mm/s and a ΔE_Q of 0.57 mm/s (0.38 mm/s line width). The parameters indicate some Fe^{3+} species which most probably originate from partial degradation of FeS clusters of NreB. Below, we will show that this component of the spectrum can be deconvoluted into a contribution from diamagnetic [2Fe-2S]$^{2+}$ clusters and a component from nonspecifically associated iron precipitates, presumably some iron oxide or hydroxide.

The anaerobic preparation of NreB contained 0.9 mol of Fe and 0.8 mol of acid labile sulfide per mole of protein (Table 2). On the basis of total Fe content and the relative abundance of FeS species in the Mössbauer spectrum, it can be estimated that 0.18 mol of [4Fe-4S]$^{2+}$/mol of NreB is present. The low contents are presumably caused by the instability of the cluster. Aerobically prepared NreB does not contain significant amounts of sulfide. Moreover, the Mössbauer spectra are very weak and do not exhibit any contribution from FeS clusters (not shown).

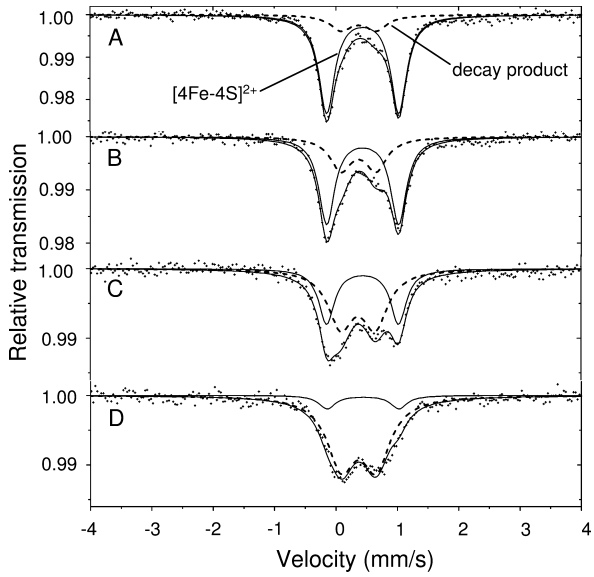

FIGURE 3: Oxygen-induced $[4Fe\text{-}4S]^{2+}$ cluster degradation monitored by Mössbauer spectroscopy. The Mössbauer spectra were recorded at 80 K from anaerobically isolated NreB (A) and show the native $[4Fe\text{-}4S]^{2+}$ cluster (isomer shift $\delta = 0.44$ mm/s, quadrupole splitting $\Delta E_Q = 1.16$ mm/s). After the sample had been exposed to air for 30 s (B), a new subspectrum appears due to oxidative cluster degradation ($\delta = 0.37$ mm/s, $\Delta E_Q = 0.57$ mm/s, 34% relative intensity). The amount of degradation product is doubled after further exposure for 120 s to O_2 (C, 61%), and after 330 s (D, 88%), the $[4Fe\text{-}4S]^{2+}$ cluster is nearly totally lost.

Effect of Air and Oxidants on NreB: Loss of the [4Fe-4S]$^{2+}$ Cluster and Formation of a [2Fe-2S]$^{2+}$ Cluster. Anaerobically prepared NreB was exposed to air in the absence of a reducing agent (DTT), and the absorption of the sample in the range from 300 to 650 nm was recorded (Figure 1). The absorbance at 325 nm decreased in biphasic kinetics within 5 min to approximately half the anaerobic value, followed by a slow decrease of the residual part within 3 h. From the absorbance at 420 nm, only a small portion (~10%) decreased in a rapid phase within 5 min, and approximately one-half of the residual absorbance decreased with very slow kinetics within 3 h.

Exposure of the anaerobic NreB to air showed a more clear-cut response when the sample was analyzed by Mössbauer spectroscopy. After exposure for 30 s, the amount of decay product which was found in a small amount in the anaerobic preparation ($\delta = 0.37$ mm/s, 17%) started to increase, and at the same time, the fraction with a δ of 0.44 mm/s corresponding to the $[4Fe\text{-}4S]^{2+}$ cluster decreased (Figure 3). The amount of decay product increased roughly inversely to the decrease in the $[4Fe\text{-}4S]^{2+}$ cluster, and after 330 s, the $[4Fe\text{-}4S]^{2+}$ cluster was mostly converted. The half-life for $[4Fe\text{-}4S]^{2+}$ cluster degradation was ~2.5 min.

Applied field measurements allowed us to further deconvolute the spectrum of the decay product of the clusters. Toward this end, a concentrated sample of anaerobically prepared NreB was inactivated by air for 5.5 min and measured first at 80 K in zero field. The spectrum which is virtually identical to that of Figure 3D could be simulated with the same two components introduced above [$\delta = 0.44$ mm/s, and $\delta \approx 0.37$ mm/s (see Figure S1 of the Supporting Information)], but the applied field measurements given in panels A and B of Figure 4 suggest alternatively three components according to (1) 12% $[4Fe\text{-}4S]^{2+}$ clusters with a δ(I) of 0.44 mm/s and a ΔE_Q(I) of 1.17 mm/s, (2) 44% of an oxidation product (II) with a characteristically low isomer shift and moderately weak quadrupole splitting [δ(II) = 0.28 mm/s, and ΔE_Q(II) = 0.57 mm/s] that are typical of $[2Fe\text{-}2S]^{2+}$ clusters, and (3) 44% of a decay product with a δ(III) of 0.50 mm/s and a ΔE_Q(III) of 0.57 mm/s. The extended fit is justified by the observation that at 4.2 K with applied fields of 0.1 and 7 T (Figure 4A,B) two well-resolved diamagnetic subspectra are observed with isomer shifts and quadrupole splittings that can be clearly assigned to subspectra I and II, having the same intensity ratio (0.27) as at 80 K with $B = 0$. The third contribution (III) apparently cannot be observed at 0.1 T due to broadening beyond detection limits, but it yields a magnetic spectrum with broad lines at approximately ±4 mm/s when a strong polarizing field of 7 T is applied (Figure 4B, not fitted). This behavior is typical of small superparamagnetic particles as they are occasionally found for contaminants in iron proteins. The strong broadening at liquid helium temperatures results from spin relaxation with rates that are size-, field-, and temperature-dependent. The isomer shift and quadrupole splitting of component III resemble those of iron oxide or hydroxide (*30*). Therefore, we assume that the component results from iron precipitates that originate from oxidative degradation. It seems to be the final decay product of the $[4Fe\text{-}4S]^{2+}$ clusters in NreB. The typically low isomer shift and moderate quadrupole splitting of component II, however, in conjunction with $S = 0$ spin, are unique features of an oxidized dinuclear $[2Fe\text{-}2S]^{2+}$ cluster; it is the only known iron−sulfur species that is diamagnetic and contains only ferric ions (*31*). The $[2Fe\text{-}2S]^{2+}$ clusters seem to be the only detectable intermediate formed upon oxidative inactivation of NreB.

Anaerobic NreB was analyzed by EPR spectrometry for the presence of paramagnetic Fe species (Figure 5). The samples were virtually EPR silent as expected for the diamagnetic $[4Fe\text{-}4S]^{2+}$ cluster. Incubation of the protein with air for increasing periods of time gave no indications of the formation of significant amounts of products or intermediates. In particular, there was no indication of the presence of a $[3Fe\text{-}4S]^{+}$ cluster ($S = {}^1/_2$, distinct narrow signals with an average g value of >2) or of a reduced $[3Fe\text{-}4S]^{0}$ cluster ($S = 2$, broad signals at low field, $g = 8-12$). A weak $g = 4.3$ signal turned up after 2 min of air treatment which is typical for contamination with nonspecific Fe^{3+} degradation products (Figure 5).

After the treatment of the anoxic NreB with air, the amounts of acid labile Fe and S^{2-} in NreB dropped (Table 2). The sample was nearly devoid of sulfide. Under the same conditions, part of the Fe was retained, but was no longer bound in a FeS cluster as concluded from the high Fe/S ratio and the lack of detectable FeS cluster. Part of the Fe might originate from the cluster and nonspecifically associate with the protein.

The Kinase Activity of NreB Depends on the [4Fe-4S]$^{2+}$ Cluster. Autophosphorylation of anaerobically prepared NreB was assessed by the incorporation of [^{33}P]phosphate from [γ-^{33}P]ATP. The protein was incubated for up to 150 s with [γ-^{33}P]ATP, and the amount of phosphate bound to NreB was measured by quantitative autoradiography following SDS−PAGE to remove phosphate which was not covalently bound to the protein (Figure 6, inset). The degree of phosphorylation increased linearly with incubation time. The

Table 2: Chemical Compositions of Aerobically and Anaerobically Prepared NreB[a]

preparation of NreB	Fe (mol/mol of NreB)	S^{2-} (mol/mol of NreB)	$[4Fe\text{-}4S]^{2+}$ (mol/mol of NreB)	$[4Fe\text{-}4S]^{2+}$ as % of total Fe
anaerobic	0.9 ± 0.17	0.8 ± 0.45	0.18	79
anaerobic, 60 min in air	0.3 ± 0.17	0.07 ± 0.03	0.02	<5
aerobic	0.3 ± 0.08	0.1 ± 0.05	nd[b]	nd[b]
aerobic, reconstituted	1.5 ± 0.31	0.7 ± 0.18	0.19	34

[a] Fe and sulfide contents were determined chemically by ferrocene (*29*) and the methylene blue method (*28*), respectively. The $[4F\text{-}4S]^{2+}$ cluster contents were derived from the chemically determined Fe content and the molar portions of the FeS cluster from total Fe as derived from Mössbauer spectra as in Figures 2 and 10. The aerobically reconstituted sample was treated in addition by gel filtration to remove nonspecifically bound ions prior to analysis. The relative content of $[Fe\text{-}4S]^{2+}$ (% of total Mössbauer detectable Fe) was derived from the experiments shown in Figures 2, 3, and 10. [b] Not detected.

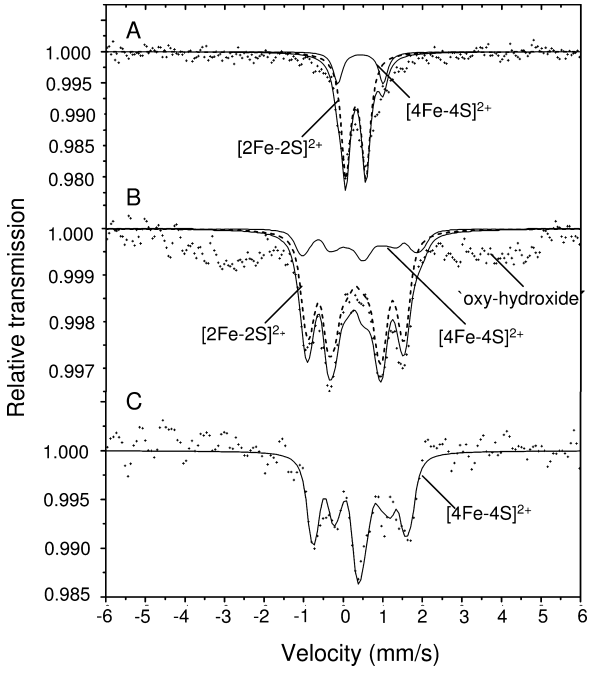

FIGURE 4: Magnetic Mössbauer spectra recorded at 4.2 K from an air-inactivated sample of NreB at 0.1 (A) and 7 T (B) and (C) from anaerobically isolated NreB at 5 T. The fields were applied perpendicular to the γ-ray, and the NreB concentration was 1.74 mM in panels A and B and 0.66 mM in panel C. The experimental spectra were additionally smoothed by a five-point Savitzky−Golay procedure (*45*). The solid lines are simulations for diamagnetic clusters ($S = 0$) with the following parameters: $\delta(I) = 0.44$ mm/s, $\Delta E_Q(I) = 1.17$ mm/s, and $\eta(I) = 0.7$, and $\delta(II) = 0.31$ mm/s, $\Delta E_Q(II) = 0.57$ mm/s, and $\eta(II) = 0.84$.

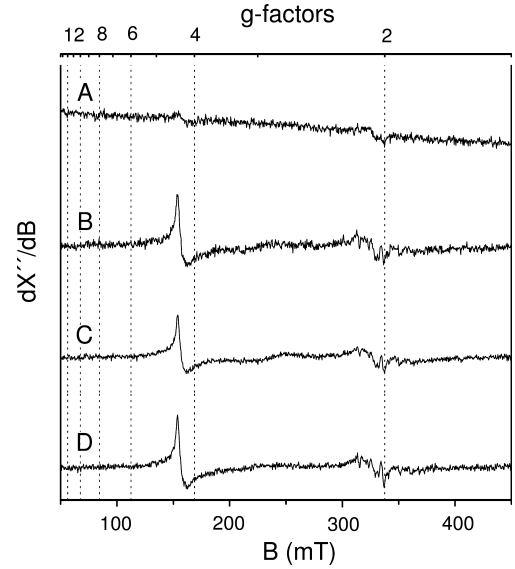

FIGURE 5: EPR spectra of anaerobically isolated NreB after exposure to air. The samples (0.53 mM NreB) were exposed to air for 30 s (A), 2 min (B), 10 min (C), and 18 min (D). The signal with the weak line at $g = 4.3$ is characteristic of nonspecifically bound Fe(III). Experimental conditions: microwave frequency, 9.4520 (A), 9.4451 (B), 9.4483 (C), and 9.4506 GHz (D); power, 0.2 mW; modulation, 1 mT/100 kHz; temperature, 10 K.

rate of autophosphorylation was highest for anaerobic NreB and decreased when the protein was incubated with air before the kinase activity was determined (Figure 6). Exposure to air decreased the phosphorylation activity to values as low as 20% of the maximum. Incubation of NreB with thiol reagents like *N*-ethylmaleimide decreased the kinase activity by more than 80% (not shown). The relative rates of autophosphorylation appeared to decrease logarithmically after the protein had been exposed to air. The air inactivation showed a half-life of ~2−3 min which was close to the rates of $[4Fe\text{-}4S]^{2+}$ cluster disassembly of anaerobic NreB and formation of degradation products of the $[4Fe\text{-}4S]^{2+}$ cluster (Figure 7), suggesting a correlation of the parameters.

Symmetry Properties and Ligands of the [4Fe-4S] Cluster of NreB. A magnetic Mössbauer spectrum was recorded from anoxically prepared NreB with an applied field of 5 T to provide definite evidence of the spin state of the FeS cluster and probe further the coordination of the Fe ions (Figure 4C). A simulation confirms the diamagnetic ground state ($S = 0$), which is expected for the $[4Fe\text{-}4S]^{2+}$ cluster. All features of the spectrum could be reasonably well fitted with a single set of Mössbauer parameters; in particular, the sign and the asymmetric parameter of the quadrupole interaction were found to be unique ($\Delta E_Q = 1.16$ mm/s, at 4.2 K, and $\eta = 0.7$). Hence, within the spectral resolution, all iron sites yield equal contributions to the magnetically perturbed spectrum. This is characteristic of a diamagnetic, symmetric $[4Fe\text{-}4S]^{2+}$ cluster with full valence delocalization.

The uniform isomer shift and quadrupole interaction suggest in particular that the four Fe ions of the cluster are bound by four sulfur ligands each, which means that the ligands provided by the protein should be the four Cys residues of NreB. For experimental proof, each of the four Cys residues of NreB was probed by mutagenic replacement with a Ser (or Ala) residue. The mutant genes were introduced on plasmid as part of the *nreABC* gene cluster into a chromosomal *nreABC* deletion strain. The complete *nreABC* operon (and mutant forms thereof) was supplied for complementation to avoid polar effects on *nreC* which could arise from deletion of *nreB* and complementation of *nreB* without the operon context. Function of NreB was tested in vivo by measuring the anaerobic growth of the bacteria with nitrate as the acceptor, and nitrate reduction (Figure 8). The loss of growth on nitrate by *nreABC* deletion strain m1 was

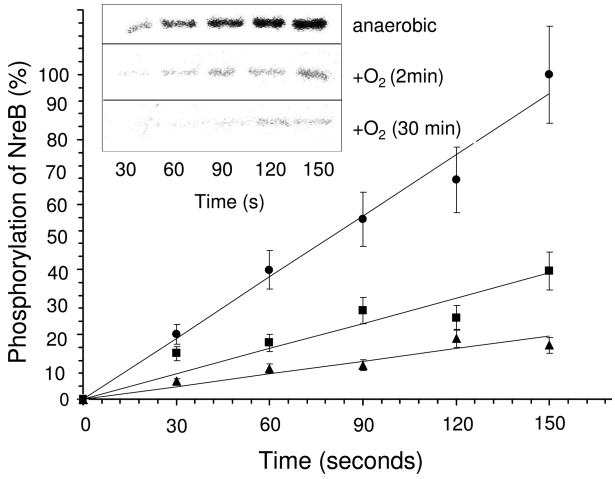

FIGURE 6: Effect of air exposure of anaerobically prepared NreB on autophosphorylation by [γ-^{33}P]ATP. Phosphorylation of anaerobically isolated NreB (0.18 mM) before (●) and after exposure for 2 (■) and 30 min (▲) to air. NreB was then incubated in reaction buffer with [γ-^{33}P]ATP at room temperature. At the indicated time points, samples were taken, quenched with SDS sample buffer, subjected to gel electrophoresis, and evaluated for radioactivity by phosphoimaging (inset). For quantitative analysis, Gel-Pro Analyzer 6.0 was used. Phosphorylation of anaerobically isolated NreB after 150 s was set to 100%.

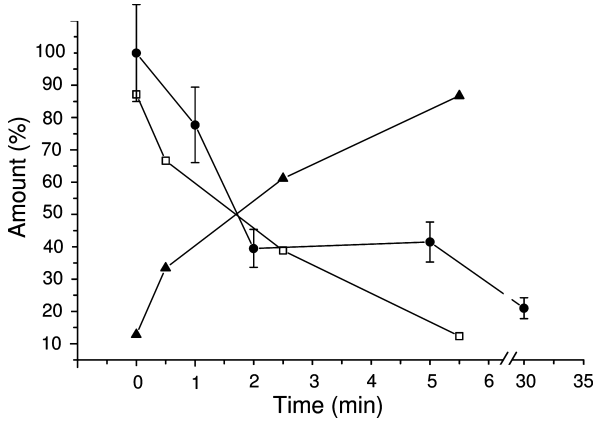

FIGURE 7: Contents of $[4Fe\text{-}4S]^{2+}$ cluster and decay poducts, and phosphorylation (kinase activity) of NreB after treatment of anaerobically prepared NreB with increasing time with air. The relative contents of the $[4Fe\text{-}4S]^{2+}$ cluster (□) and decay product (▲) were derived from Mössbauer spectroscopy as in Figures 2 and 3 and phosphorylation (●) from experiments described in the legend of Figure 6.

fully restored by complementation with the *nreABC* genes on the plasmid, whereas the plasmids encoding cysteine mutants of NreB (NreB-C59A and NreB-C74S) were not able to restore anaerobic growth on nitrate (Figure 8A). The same was observed for plasmids supplying mutant forms NreB-C62S and NreB-C77S (not shown). Nitrate and nitrite reduction was tested by measuring the level of formation and consumption of nitrite (Figure 8B) which depends on a membrane-bound nitrate and a cytoplasmic nitrite reductase (*32*). Expression of nitrate and nitrite reductases is known to depend on a functional NreB protein (*18*). In the wild type and the strain complemented with wild-type *nreABC*, nitrite was formed and accumulated in the medium. After conversion of most (≥70%) of the nitrate to nitrite, the nitrite was degraded by both strains (Figure 8B). In the complemented strain, nitrite formation and degradation started and were complete ~2.5 h later than in the chromosomal wild

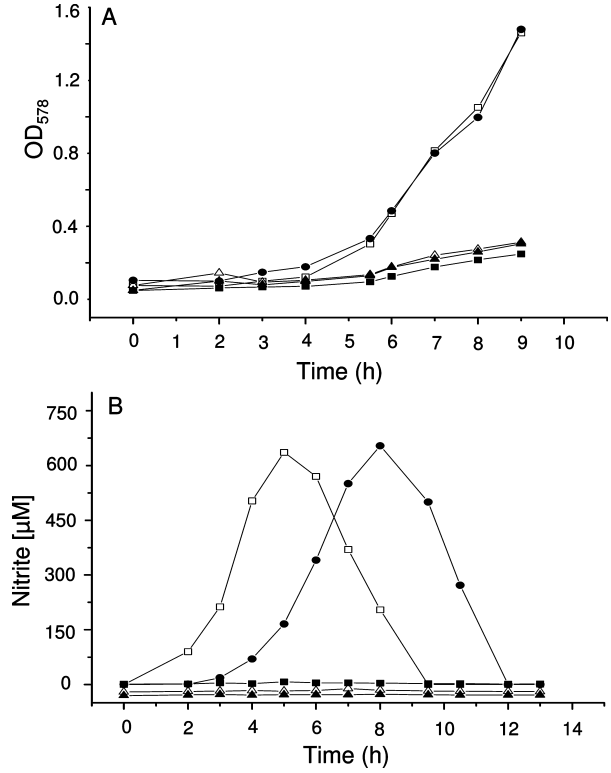

FIGURE 8: Anaerobic growth of *S. carnosus* nreB mutants in the presence of nitrate (A) and nitrite production from nitrate (B). (A) Wild-type *S. carnosus* (□) and strain m1 (*ermB*::*nreABC*) (■) and transformants of strain m1 with plasmid pRB473*nreABC* (●), plasmid pRB473*nreAB*$_{C59A}$*C* encoding NreB-C59A (▲), or plasmid pRB473*nreAB*$_{C74S}$C encoding NreB-C74S (△) were grown in BM medium with 1 mM nitrate under anaerobic conditions. (B) Nitrite formation and nitrite consumption are given for growth of the same strains of *S. carnosus* in BM medium with 1 mM nitrate.

type, but the rate of conversion is approximately the same as in the wild type. The plasmids encoding the *nreB* Cys mutants as part of the *nreABC* operon, on the other hand, were not able to complement nitrite formation and degradation [NreB-C59A or NreB-C77S (Figure 8B) and NreB-C62S and NreB-C787S (not shown)]. The mutants therefore confirm the need for each of the Cys residues for the function of NreB.

Accessibility of the [4Fe-4S]$^{2+}$ Cluster of NreB to Reduction? The $[4Fe\text{-}4S]^{2+}$ cluster of NreB "as prepared" is diamagnetic and showed no EPR spectrum, as expected (not shown). Therefore, the response of the cluster to reduction could be sensitively tested by EPR spectroscopy; the one-electron reduced state (1+) should show an $S = {}^1/_2$ state. In a first experiment, anaerobic NreB was incubated under anaerobic conditions with deazaflavin which can be cleaved with light to yield a strong electronegative reductant (at most −650 mV) (*25*). Upon illumination of the assay, the magnitudes of the bands at A_{325} and A_{420} in the absorption spectrum of NreB decreased in a very slow reaction and were mostly lost after 30 min (Figure 9A). Reduction by dithionite caused even slower bleaching of the absorption shoulder. The bleaching could be an indication of the reduction of the FeS cluster (*9*) or of degradation of the cluster following reduction.

After photoreduction for 5 min, the EPR spectrum of anaerobic NreB shows only some very weak and rather nonspecific signals at g values of ~2.8, ~2.06, ~1.87, and

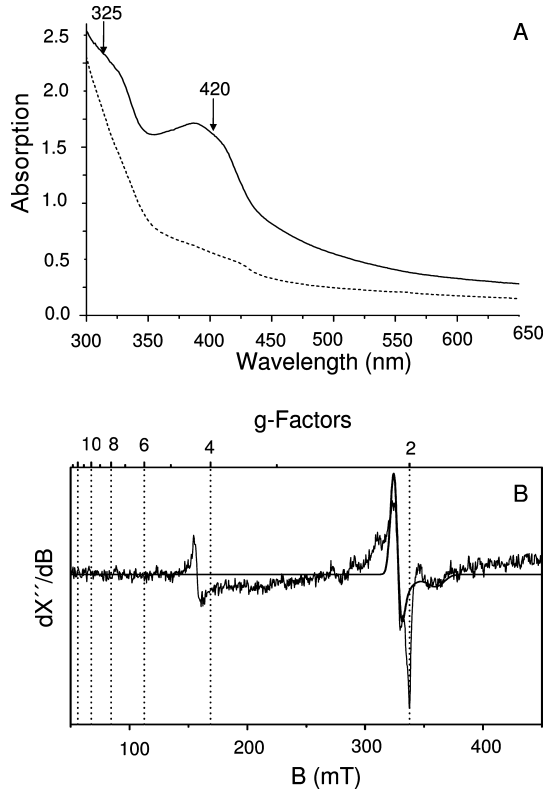

FIGURE 9: Effect of photoreduction of anaerobic NreB·[4Fe-4S]$^{2+}$ by deazaflavin on the absorption (A) and EPR spectrum (B). (A) Anaerobically prepared NreB (0.42 mM, solid line) was photoreduced in the presence of deazaflavin (41 μM) for 30 min (dotted line). (B) The anaerobically prepared NreB (0.9 mM) was photoreduced in the presence of deazaflavin for 5 min, and the EPR spectrum was recorded at 9.4502 GHz, 0.2 mW, and 10 K. The simulation represents a powder spectrum with $g = 1.87$.

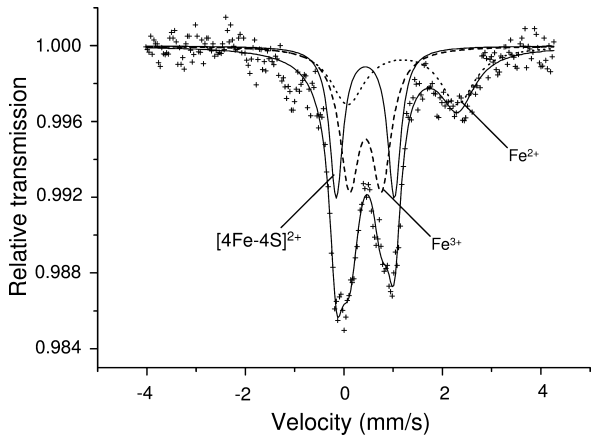

FIGURE 10: Mössbauer spectra at 80 K from in vitro reconstituted NreB. The labeled traces are simulated subspectra of the experimental spectrum, which are assigned to the [4Fe-4S]$^{2+}$ clusters (isomer shift $\delta = 0.44$ mm/s, and quadrupole splitting $\Delta E_Q = 1.17$ mm/s), "free", non-cluster-bound ferric iron (isomer shift $\delta = 0.44$ mm/s, and quadrupole splitting $\Delta E_Q = 0.64$ mm/s), and nonspecifically bound ferrous iron (isomer shift $\delta = 1.19$ mm/s, and quadrupole splitting $\Delta E_Q = 2.22$ mm/s).

~1.86 (Figure 9B). Only the line at $g = 1.87$ may be assigned to the formation of a minute amount of a [4Fe-4S]$^{+}$ or [2Fe-2S]$^{+}$ cluster (*33*). However, the other g values of the corresponding spectrum cannot be safely identified. Therefore, the provisional simulation shown in Figure 9B is just meant to guide the eye. Prolonged photoreduction also did not yield sizable amounts of any EPR spectrum characteristic of a reduced FeS cluster (not shown).

Dithionite reduction of NreB·[4Fe-4S]$^{2+}$ for 5 min caused no change in the amount and properties of the [4Fe-4S]$^{2+}$ cluster. More extended exposure of NreB·[4Fe-4S]$^{2+}$ to 10 mM dithionite, however, caused bleaching of the protein and EPR signals at $g > 2$. Correspondingly, also in the Mössbauer spectra, the formation of decay products was not observed at low concentrations of dithionite. Instead, however, a new spectrum appeared that is typcial of N- or O-liganded Fe^{2+} ($\delta = 1.28$ mm/s, and $\Delta E_Q = 2.20$ mm/s). The abundance of the species (14% of total iron) was similar to that of the degradation products found in the anaerobically prepared sample, suggesting that the Fe^{2+} apparently replaces the decay products.

Overall, it appears from UV−vis, EPR, and Mössbauer spectra that the [4Fe-4S]$^{2+}$ cluster is slowly reduced in the presence of very strong reducing agents like photoreduced deazaflavin. The reduced cluster, however, is not stable and degrades spontaneously within seconds, so that it cannot be trapped in sizable amounts.

NreB Is a Permanent Dimer. An anaerobic preparation of NreB containing [4Fe-4S]$^{2+}$ was subjected to size-exclusion chromatography under anaerobic conditions. The sample eluted in a band with a volume corresponding to a protein of 84 kDa (Figure 2 of the Supporting Information). After being exposed to air, the sample had an elution volume very similar to that of a 98 kDa protein. Therefore, both forms of NreB are homodimers of the monomer (40.0 kDa). In addition to the protein band of dimeric NreB, there were varying amounts of a second form consisting of NreB protein with an apparent M_r of >600 kDa, suggesting that part of the protein aggregates.

Reconstitution of a [4Fe-4S]$^{2+}$ Cluster in ApoNreB. Aerobically prepared NreB contained no significant amount of acid labile sulfide (Table 2) and showed no spectral indication of FeS clusters. We tried to reconstitute FeS clusters in the apoprotein by using an established in vitro procedure which was as used for FNR and NreB previously (*9, 15, 19*). In this procedure, sulfide ions are supplied by cysteine desulfurase from cysteine and Fe(II) ions by the redox-stabile Mohr's salt, $(NH_4)_2[Fe(H_2O)_6](SO_4)_2$. Here $(NH_4)_2[^{57}Fe(H_2O)_6](SO_4)_2$ was used to incorporate ^{57}Fe into the FeS clusters. The reconstituted NreB exhibited an UV−vis absorption spectrum with shoulders at 350 and 420 nm similar to that of anaerobically prepared NreB. After removal of nonbound low-molecular mass components by gel filtration, the Fe and sulfide contents were approximately one per mole of NreB (Table 2). The Mössbauer spectrum (Figure 10) could be simulated by superimposition of three spectra that were characteristic of the [4Fe-4S]$^{2+}$ cluster, the degradation products known from air-exposed anaerobic NreB, and noncluster Fe^{2+}. The [4Fe-4S]$^{2+}$ cluster contained approximately one-third of the total iron, and the decay products and Fe^{2+} fractions contained slightly more (39%) and less (29%), respectively. No indications for other components were obtained. Therefore, reconstitution of NreB resulted in incorporation of the [4Fe-S]$^{2+}$ cluster, and the other compounds are presumably remnants of the reconstitution procedure or degradation products. Nonspecific but tightly adhering Fe ions are often difficult to remove from proteins by gel filtration or other methods without denaturing

the protein. From the Fe and related $[4Fe\text{-}4S]^{2+}$ cluster contents, we can estimate that 0.12 mol of $[4Fe\text{-}4S]^{2+}$ cluster is incorporated per mole of reconstituted NreB.

Reconstituted NreB·$[4Fe\text{-}4S]^{2+}$ gained kinase activity (not shown) which was absent in the aerobically prepared NreB. The reconstitution of the kinase activity by incorporation of the FeS cluster supports the view that the presence of the $[4Fe\text{-}4S]^{2+}$ cluster in NreB is an essential prerequisite for kinase activity. Obviously, NreB per se provides the properties for specific binding and formation of a $[4Fe\text{-}4S]^{2+}$ cluster.

DISCUSSION

Oxygen Sensitivity of the $[4Fe\text{-}4S]^{2+}$ Cluster in Anaerobic NreB. The native FeS cluster in anaerobic NreB is a diamagnetic $[4Fe\text{-}4S]^{2+}$ cubane according to all the criteria that have been applied. Up to 0.19 mol of the $[4Fe\text{-}4S]^{2+}$ cluster was detected in NreB. In FNR, a content of 0.5−0.76 mol of the same cluster type was found (*7*). Direct evidence came from Mössbauer spectroscopy which showed the presence of mixed-valence Fe(II/III)S_4 sites and diamagnetic behavior ($S = 0$). Moreover, the redox properties are also typical for $[4Fe\text{-}4S]^{2+}$ clusters of the type found in *E. coli* FNR. The significance of the $[4Fe\text{-}4S]^{2+}$ cluster is confirmed by the presence of the same cluster type upon reconstitution of apoNreB in vitro and the concomitant gain in kinase activity. The cluster does not function as a redox mediator as in electron transfer proteins, and it is reduced only at a very low redox potential ($E_0 \leq -650$ mV). Reaction with O_2 therefore does not cause a reversible redox reaction but is the starting point for degradation of the cluster. The properties of the cluster are compatible with those of other FeS clusters used for O_2 sensing (*3, 6*). The $[4Fe\text{-}4S]^{2+}$ cluster of NreB is liganded by four Cys residues as shown by the uniform appearance of the magnetic Mössbauer spectrum and the mutation analysis.

Incubation of $[4Fe\text{-}4S]^{2+}$·NreB with O_2 yields small amounts of high-spin Fe(III) species with rhombic EPR signals, and later a $[2Fe\text{-}2S]^{2+}$ cluster and γ-FeOOH-like degradation products appear (Figure 11). The $[2Fe\text{-}2S]^{2+}$ cluster is the major first degradation product with a significant half-life. Thus, the primary response of the $[4Fe\text{-}4S]^{2+}$ cluster-containing O_2 sensors NreB and FNR to O_2 is the same, i.e., conversion of the $[4Fe\text{-}4S]^{2+}$ cluster to a $[2Fe\text{-}2S]^{2+}$ cluster, and even the kinetics appears to be similar, although the clusters are found in different types of proteins. The final product of air inactivation of NreB is apoNreB, and the same form of NreB is obtained when the protein is isolated from aerobically grown bacteria, or after isolation under aerobic conditions. The kinetics of $[2Fe\text{-}2S]^{2+}$ formation and degradation in NreB, however, have not been resolved. Similar to FNR, the $[2Fe\text{-}2S]^{2+}$ cluster-containing form of NreB is inactive. The consequences of the $[4Fe\text{-}4S]^{2+}$ to $[2Fe\text{-}2S]^{2+}$ conversion on the mode of protein function are different for FNR and NreB. In FNR, the conversion controls dimerization (and DNA binding), whereas NreB is a permanent dimer similar to FNR_{Bs}. In NreB, the FeS cluster controls kinase activity.

Only for FNR of *E. coli* have the reactions at the FeS cluster been determined in detail. The $[4Fe\text{-}4S]^{2+}$ cluster is converted via an intermediate, a $[3Fe\text{-}4S]^{+}$ cluster, to FNR with a $[2Fe\text{-}2S]^{2+}$ cluster. The cluster conversion is coupled

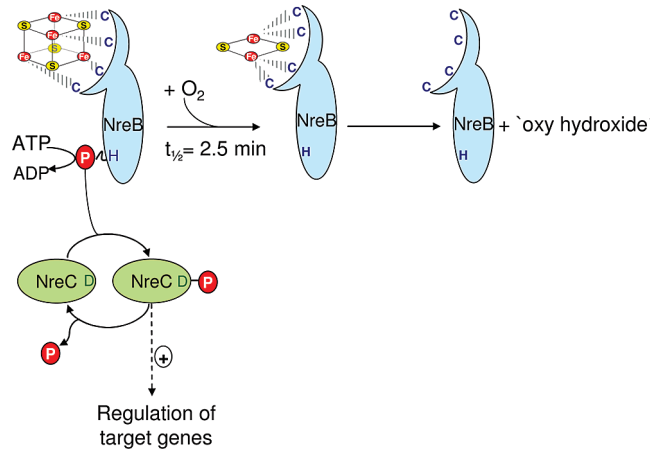

FIGURE 11: Scheme for the function of the NreBC two-component system. For NreB, the kinase domain with the conserved His (H) residue and the PAS domain with the conserved Cys residues (C) are shown. $[4Fe\text{-}4S]^{2+}$·NreB and apoNreB are shown which were identified by biochemical and spectroscopic assays. The half-life $t_{1/2}$ for interconversion under air at room temperature in vitro is 2.5 min. The anaerobic $[4Fe\text{-}4S]^{2+}$·NreB has high kinase activity, resulting in the phosphorylation of NreB and NreC. NreC-P activates transcription of target genes *narGHJI*, *narT*, and *nirBD*.

to the release of one Fe(II) and one Fe(III) (*22, 24*). Degradation of the $[2Fe\text{-}2S]^{2+}$ cluster during conversion to apoFNR releases formally two Fe(III) ions, but it is not clear whether the iron is released as Fe(II) or Fe(III) or whether all Fe is released (*34*). In NreB, $[3Fe\text{-}4S]^{+}$ cluster formation was not observed so far. Further studies on the kinetics of $[2Fe\text{-}2S]^{2+}$ cluster formation and degradation will shed more light on the role of the FeS cluster in NreB function.

The Sensory Domain of NreB Is a $[4Fe\text{-}4S]^{2+}$ Cluster-Containing PAS Domain. For the sensory domain of NreB, all features that are typical for PAS domains (*35, 36*) can be predicted (Figure 12). The domain starts with an α-helical N-terminal cap (amino acids 1−21) which is followed by the PAS core (amino acids 24−61) with two β sheets and two α helices. A third α helix (amino acids 46−55) typical for PAS cores was predicted with lower probability. The core is linked by a loop (amino acids 64−67) to the helical connector (amino acids 67−82) and the β scaffold (amino acids 88−123). The scaffold consists of three β sheets which are linked by short loops. The middle β sheet has the lowest probability. A summary of the predicted secondary structures is given in Figure 12C. The essential Cys residues of NreB are located at the C-terminal end of the last α helix of the PAS core (C59 and C62) and in the helical connector (C74 and C77).

The PAS domain of NreB is related in sequence to heme B-binding PAS domains of the sensor kinase FixL from *R. meliloti* (31% identical in sequence to the PAS domains) and *Br. japonicum* (27% identical). FixL sensor kinases control the expression of N_2 fixation genes in response to O_2 (*37*). Structural and functional aspects of O_2 sensing by FixL are well-characterized. A His residue (His194 in *R. meliloti* FixL) from the connector helix of the PAS domain represents the fifth (axial) ligand of the Fe(II) in heme B (*38*). After binding of O_2 as the sixth ligand, the Fe ion shifts from the high- to low-spin Fe(II) state. The changed binding is transmitted by an Arg and the His residue via the connector helix and the β scaffold to the kinase domain, resulting in the inactivation

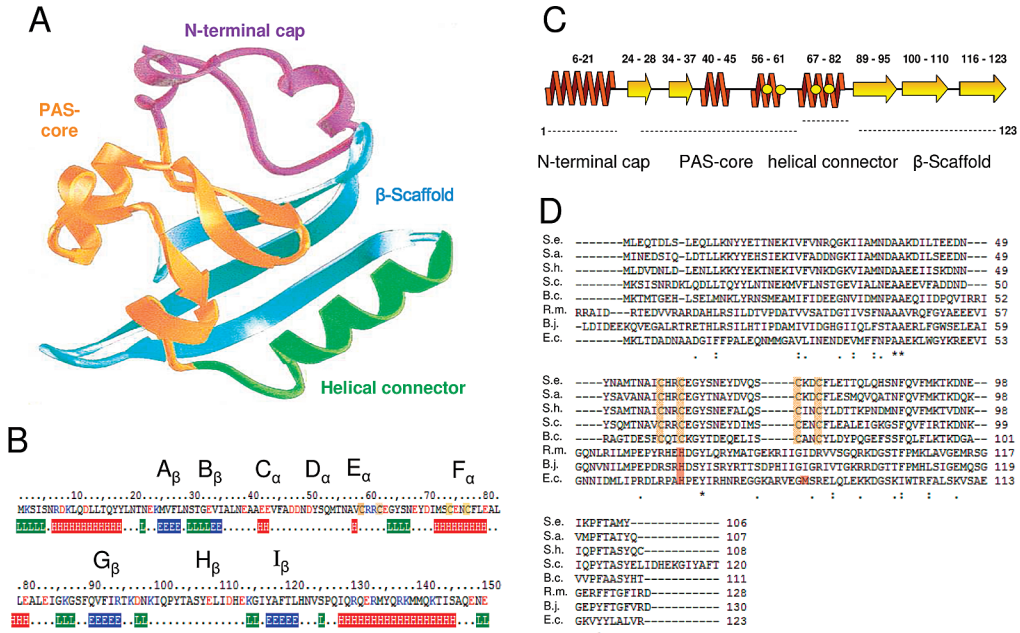

FIGURE 12: Properties of the sensory PAS domain of NreB. (A) General structure of PAS domains consisting of the N-terminal cap, core, β scaffold, and helical connector regions. (B) Secondary structure prediction for the PAS domain of NreB (amino acids 1−150) according to the PredictProtein server (*46*). The top line gives the secondary structural elements, the second line the numbering of the protein sequence, the third line the sequence, and the bottom line helical (H), β sheet (E), and loop (L) structure predictions with high probability (>5). (C) Summary of secondary structure predictions of the PAS domain of NreB for regions with high probability. The positions of the essential Cys residues (C59, C62, C74, and C77) are indicated. (D) Multiple-sequence alignment of O_2-sensing PAS domains of the $[4Fe\text{-}4S]^{2+}$ cluster-binding NreB proteins of *Staphylococcus epidemidis* (S.e.), *Staphylococcus aureus* (S.a.), *Staphylococcus hemolyticus* (S.h.), *S. carnosus* (S.c.), and *Bacillus clausii* (B.c.), of the heme B-binding PAS domains of FixL from *Rhizobium meliloti* (R.m.) and *Bradyrhizobium japonicum* (B.j.), and of Dos from *E. coli* (E.c.).

of the kinase. Cys62 of NreB is at a position homologous to that of the His residue of FixL in the connector helix, which could be an indication that structural changes induced by $[4Fe\text{-}4S]^{2+}$ cluster decay are transmitted to the connector helix and the kinase domain of NreB.

The Dos sensor of *E. coli* contains a heme B-binding PAS domain for controlling cyclic di-GMP phosphodiesterase activity of the protein in response to O_2 (*39*−*41*). The PAS domain is similar in sequence to NreB (21% identical). The His residue serving in FixL as the proximal ligand for heme B is conserved in the PAS domain of Dos as well (see Figure 12C). Dos contains in addition a distal Met ligand (Met87) at the O_2 site of heme B which is displaced after O_2 binding. Met87 is positioned very close to the Cys74/Cys77 pair of NreB which further strengthens the analogy of heme B and $[4Fe\text{-}4S]^{2+}$ cluster binding by the PAS domains of FixL, Dos, and NreB (Figure 12D).

Overall, it appears that NreB binds the O_2-sensitive $[4Fe\text{-}4S]^{2+}$ cluster by a PAS domain. The $[4Fe\text{-}4S]^{2+}$ clusters in FNR and NreB are very similar in structure and function, but the corresponding proteins are not related. The Cys clusters which bind the $[4Fe\text{-}4S]^{2+}$ clusters in both proteins show no similarity in sequence and spacing of the Cys residues, suggesting that the clusters have been acquired independently for the same purpose by different proteins.

NreB Proteins in Gram-Positive Bacteria. Screening for NreB homologues revealed NreB-like proteins outside the *Staphylococcus* group (Figure 13A). *Bacillus clausii* encodes a sensor kinase with a high degree of sequence similarity to NreB of *S. carnosus* (55% identical), including the four essential Cys residues (Swiss-Prot/TrEMBL). *nreB* of *B. clausii* is part of a *nreABC* gene cluster that is located next to the *narGHJI* and *narT* genes. The similarity in sequence and gene context suggests that NreBC of *B. clausii* has a function similar to that of *S. carnosus*. *B. clausii* lacks a protein similar to FNR_{Bs} which controls expression of the *narGHJI* and *narT* genes in *B. subtilis* and other *Bacillus* strains.

B. amyloliquefaciens encodes a putative sensor kinase that is similar to NreB of *S. carnosus* (31% identical in the PAS domain). Only three of the Cys residues are conserved in the predicted protein. The gene is accompanied by a gene similar to *nreC* but lacks a *nreA*-like gene. The *narGHJI* and *narT* genes of *B. amyloliquefaciens* are located adjacent to a *fnr*-like gene as in *B. subtilis*, suggesting that the genes encoding the histidine kinase and the response regulator are not homologous in function to *nreBC* of *S. carnosus*.

Lactobacillus plantarum and *Lactobacillus reuteri* encode sensory His kinases that are 28 and 27% identical to the PAS domain of *S. carnosus*, respectively (Swiss-Prot/TrEMBL). For the PAS proteins, typical secondary structures are predicted, but the *Lactobacillus* proteins contain only the C-terminal pair of Cys residues (homologous to Cys74 and Cys77 of NreB). The genes are accompanied by genes that are similar to *nreC* and *nreA* in *L. plantarum* and *nreC* in *L. reuteri*, suggesting the presence of NreBC-type two-component systems. The finding of NreB homologues with two Cys residues is reminiscent of the Flp (FNR-like proteins) in *Lactobacillus casei* and *Lactococcus lactis*. The Flp proteins are similar in sequence to FNR/CRP but carry only two of the four essential Cys residues of FNR (*42, 43*). The functional state of Flp from *L. casei* is regulated by a thiol−disulfide interconversion in response to O_2, whereas FlpA from *L. lactis* is a FeS cluster-based O_2 sensor despite

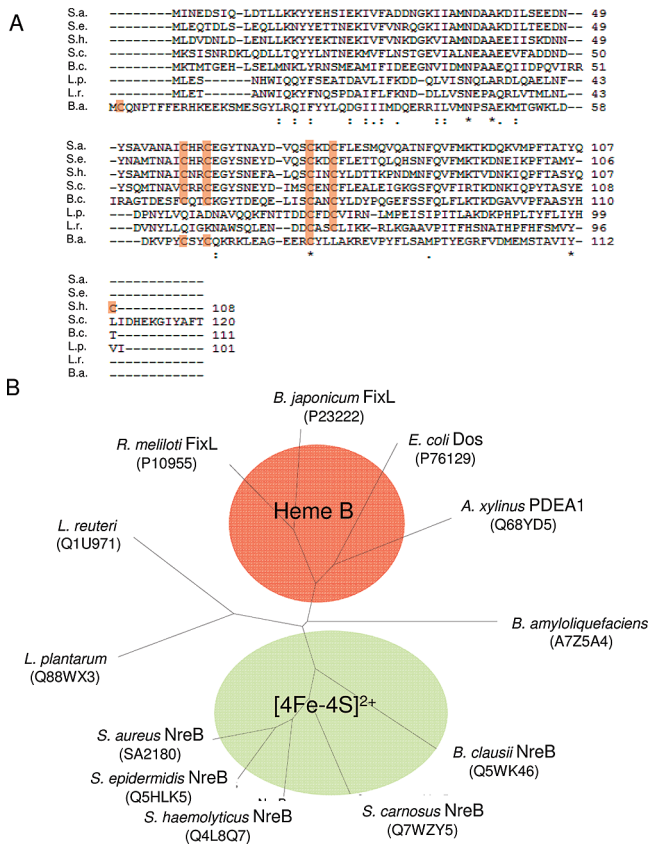

FIGURE 13: NreB-like proteins. (A) Sequence comparison of the PAS domain of NreB from *S. aureus* (S.a.), *S. epidermidis* (S.e.), *S. hemolyticus* (S.h.), *S. carnosus* (S.c.), and *B. clausii* (B.c.), the NreB like proteins from *Lactobacillus plantarum* (L.p.) and *Lactobacillus reuteri* (L.r.), and a sensor kinase of *Bacillus amyloliquefaciens* (B.a.). For sequence alignment, ClustalW 2.0.5 (*47*) was used. Conserved Cys residues are highlighted in orange, conserved residues denoted with asterisks, and conservatively and semiconservatively exchanged residues denoted with colons and periods, respectively. (B) Phylogenetic tree of the $[4Fe\text{-}4S]^{2+}$ cluster and the heme B-binding PAS domains of the NreB, FixL, and Dos proteins (accession numbers in parentheses). The phylogenetic tree was calculated from the multiple alignments of panels A and of Figure 12D with the neighbor-joining method (*48*) with ClustalW and displayed by TreeView (version 1.5.2).

the presence of only two Cys residues per monomer. The *nreBC* homologues of the *Lactobacillus* strains are accompanied by *nar* genes of nitrate respiration and the *moe* operon encoding proteins for molybdopterine cofactor biosynthesis, suggesting that the NreBC homologues control nitrate respiration in the *Lactobacillus* strains. The PAS domains of the NreB (and NreB-like) and heme B-binding proteins (Figure 13B) cluster in separate subgroups in a phylogenetic tree based on the protein sequence of the domain. The PAS domains of the NreB-like proteins form a subgroup which is separated from the NreB proteins of *Staphylococcus* and *B. clausii*. The clustering confirms the relation of the heme B- and $[4Fe\text{-}4S]^{2+}$ cluster-containing PAS domains and the suggestion that both groups use different devices for signal perception but might share similarities in the mode of transmission of the signal to the kinase domain.

ACKNOWLEDGMENT

We are grateful to A. Lupas (Universität Tübingen) for drawing our attention to the similarity of NreB to PAS proteins, F. Götz (Universität Tübingen) for the supply of strains and plasmids, F. Renz, M. Klein, and D. Hill (Universität Mainz) for help with the preparation of $(NH_4)_2{}^{57}Fe(SO_4)_2$, and Th. Selmer (Universität Marburg) for providing a sample of deazaflavin.

SUPPORTING INFORMATION AVAILABLE

Oligonucleotides used for site-directed mutagenesis and cloning (Table 1).

zero-field Mössbauer spectrum of the air-inactivated sample of NreB used in Figure 4 recorded at 80 K (Figure S1), and size-exclusion chromatography of aerobic and anaerobic NreB (Figure S2). This material is available free of charge via the Internet at http://pubs.acs.org.

REFERENCES

1. Guest, J. R. (1995) Adaption to life without oxygen. *Philos. Trans. R. Soc. London, Ser. B 350*, 189–202.
2. Unden, G., Becker, S., Bongaerts, J., Holighaus, G., Schirawski, J., and Six, S. (1995) O_2-sensing and O_2-dependent gene regulation in facultatively anaerobic bacteria. *Arch. Microbiol. 164*, 81–90.
3. Green, J., and Paget, M. S. (2004) Bacterial redox sensors. *Nat. Rev. Microbiol. 2*, 954–966.
4. Malpica, R., Franco, B., Rodriguez, C., Kwon, O., and Georgellis, D. (2004) Identification of a quinone-sensitive redox switch in the ArcB sensor kinase. *Proc. Natl. Acad. Sci. U.S.A. 101*, 13318–13323.
5. Crack, J. C., Le Brun, N. E., Thomson, A. J., Green, J., and Jervis, A. J. (2008) Reactions of Nitric Oxide and Oxygen with the Regulator of Fumarate and Nitrate Reduction, a Global Transcriptional Regulator, during Anaerobic Growth of *Escherichia coli*. *Methods Enzymol. 437*, 191–209.
6. Kiley, P. J., and Beinert, H. (2003) The role of Fe-S proteins in sensing and regulation in bacteria. *Curr. Opin. Microbiol. 6*, 181–185.
7. Khoroshilova, N., Popescu, C., Münck, E., Beinert, H., and Kiley, P. J. (1997) Iron-sulfur cluster disassembly in the FNR protein of *Escherichia coli* by O_2: [4Fe-4S] to [2Fe-2S] conversion with loss of biological activity. *Proc. Natl. Acad. Sci. U.S.A. 94*, 6087–6092.
8. Lazazzera, B. A., Beinert, H., Khoroshilova, N., Kennedy, M. C., and Kiley, P. J. (1996) DNA binding and dimerization of the FeS-containing FNR Protein from *Escherichia coli* are regulated by oxygen. *J. Biol. Chem. 271*, 2762–2768.
9. Green, J., Bennett, B., Jordan, P., Ralph, E. T., Thomson, A. J., and Guest, J. R. (1996) Reconstitution of the [4Fe-4S] cluster in FNR and demonstration of the aerobic-anaerobic transcription switch *in vitro*. *Biochem. J. 316*, 887–892.
10. Becker, S., Holighaus, G., Gabrielczyk, T., and Unden, G. (1996) O_2 as the regulatory signal for FNR-dependent gene regulation in *Escherichia coli*. *J. Bacteriol. 178*, 4515–4521.
11. Unden, G., and Schirawski, J. (1997) The oxygen-responsive transcriptional regulator FNR of *Escherichia coli*: The search for signals and reactions. *Mol. Microbiol. 25*, 205–210.
12. Crack, J., Green, J., and Thomson, A. J. (2004) Mechanism of oxygen sensing by the bacterial transcription factor fumarate-nitrate reduction (FNR). *J. Biol. Chem. 279*, 9278–9286.
13. Crack, J. C., Green, J., Cheesman, M. R., Le Brun, N. E., and Thomson, A. J. (2007) Superoxide-mediated amplification of the oxygen-induced switch from [4Fe-4S] to [2Fe-2S] clusters in the transcriptional regulator FNR. *Proc. Natl. Acad. Sci. U.S.A. 104*, 2092–2097.
14. Sutton, V. R., Mettert, E. L., Beinert, H., and Kiley, P. J. (2004) Kinetic analysis of the oxidative conversion of the $[4Fe\text{-}4S]^{2+}$ cluster of FNR to a $[2Fe\text{-}2S]^{2+}$ cluster. *J. Bacteriol. 186*, 8018–8025.
15. Reinhart, F., Achebach, S., Koch, T., and Unden, G. (2008) Reduced apo-fumarate nitrate reductase regulator (apoFNR) as the major form of FNR in aerobically growing *Escherichia coli*. *J. Bacteriol. 190*, 879–886.
16. Reents, H., Gruner, I., Harmening, U., Böttger, L. H., Layer, G., Heathcote, P., Trautwein, A. X., Jahn, D., and Härtig, E. (2006) *Bacillus subtilis* FNR senses oxygen via a [4Fe-4S] cluster

coordinated by three cysteine residues without change in the oligomeric state. *Mol. Microbiol. 60*, 1432–1445.
17. Reents, H., Münch, R., Dammeyer, T., Jahn, D., and Härtig, E. (2006) The Fnr regulon of *Bacillus subtilis*. *J. Bacteriol. 188*, 1103–1112.
18. Fedtke, I., Kamps, A., Krismer, B., and Götz, F. (2002) The nitrate reductase and nitrite reductase operons and the narT gene of *Staphylococcus carnosus* are positively controlled by the novel two-component system NreBC. *J. Bacteriol. 184*, 6624–6634.
19. Kamps, A., Achebach, S., Fedtke, I., Unden, G., and Götz, F. (2004) Staphylococcal NreB: An O_2-sensing histidine protein kinase with an O_2-labile iron-sulphur cluster of the FNR type. *Mol. Microbiol. 52*, 713–723.
20. Wieland, K. P., Wieland, B., and Götz, F. (1995) A promoter-screening plasmid and xylose-inducible, glucose-repressible expression vectors for *Staphylococcus carnosus*. *Gene 158*, 91–96.
21. Kempf, M., Theobald, U., and Fiedler, H.-P. (1999) Economic improvement of the fermentative production of gallidermin by *Staphylococcus gallinarum*. *Biotechnol. Lett. 21*, 663–667.
22. Niehaus, F., Hantke, K., and Unden, G. (1991) Iron content and FNR-dependent gene regulation in *Escherichia coli*. *FEMS Microbiol. Lett. 84*, 319–324.
23. Shima, S., Lyon, E. J., Thauer, R. K., Mienert, B., and Bill, E. (2005) Mössbauer studies of the iron-sulfur cluster-free hydrogenase: The electronic state of the mononuclear Fe active site. *J. Am. Chem. Soc. 127*, 10430–10435.
24. Götz, F., and Schumacher, B. (1987) Improvement of protoplast transformation in *Staphylococcus carnosus*. *FEMS Microbiol. Lett. 40*, 285–288.
25. Hemmerich, P., and Massey, V. (1977) Flavin and 5-deazaflavin: A chemical evaluation of 'modified' flavoproteins with respect to the mechanisms of redox biocatalysis. *FEBS Lett. 84*, 5–21.
26. Brückner, R. (1992) A series of shuttle vectors for *Bacillus subtilis* and *Escherichia coli*. *Gene 122*, 187–192.
27. Nicholas, D. J. D., and Nason, A. (1957) Determination of nitrate and nitrite. *Methods Enzymol. 3*, 981–984.
28. Siegel, L. M. (1965) A Direct Microdetermination for Sulfide. *Anal. Biochem. 11*, 126–132.
29. Fish, W. W. (1988) Rapid colorimetric micromethod for the quantitation of complexed iron in biological samples. *Methods Enzymol. 158*, 357–364.
30. Greenwood, N. N., and Gibb, T. C. (1971) *Mössbauer Spectroscopy*, Chapman and Hall Ltd., London.
31. Beinert, H., Holm, R. H., and Münck, E. (1997) Iron-sulfur clusters: Nature's modular, multipurpose structures. *Science 277*, 653–659.
32. Neubauer, H., Pantel, I., and Götz, F. (1999) Molecular characterization of the nitrite-reducing system of *Staphylococcus carnosus*. *J. Bacteriol. 181*, 1481–1488.
33. Hughes, M. N., and Poole, R. K. (1989) *Metals and Microorganisms*, Chapman and Hall Ltd., London.
34. Sutton, V. R., Stubna, A., Patschkowski, T., Münck, E., Beinert, H., and Kiley, P. J. (2004) Superoxide destroys the $[2Fe\text{-}2S]^{2+}$ cluster of FNR from *Escherichia coli*. *Biochemistry 43*, 791–798.
35. Taylor, B. L., and Zhulin, I. B. (1999) PAS domains: Internal sensors of oxygen, redox potential, and light. *Microbiol. Mol. Biol. Rev. 63*, 479–506.
36. Vreede, J., van der Horst, M. A., Hellingwerf, K. J., Crielaard, W., and van Aalten, D. M. (2003) PAS domains. Common structure and common flexibility. *J. Biol. Chem. 278*, 18434–18439.
37. Gilles-Gonzalez, M. A., and Gonzalez, G. (2005) Heme-based sensors: Defining characteristics, recent developments, and regulatory hypotheses. *J. Inorg. Biochem. 99*, 1–22.
38. Miyatake, H., Mukai, M., Park, S. Y., Adachi, S., Tamura, K., Nakamura, H., Nakamura, K., Tsuchiya, T., Iizuka, T., and Shiro, Y. (2000) Sensory mechanism of oxygen sensor FixL from *Rhizobium meliloti*: Crystallographic, mutagenesis and resonance Raman spectroscopic studies. *J. Mol. Biol. 301*, 415–431.
39. Delgado-Nixon, V. M., Gonzalez, G., and Gilles-Gonzalez, M. A. (2000) Dos, a heme-binding PAS protein from *Escherichia coli*, is a direct oxygen sensor. *Biochemistry 39*, 2685–2691.
40. Kurokowa, H., Lee, D. S., Watanabe, M., Sagami, I., Mikami, B., Raman, C. S., and Shimizu, T. (2004) A redox-controlled molecular switch revealed by the crystal structure of a bacterial heme PAS sensor. *J. Biol. Chem. 279*, 20186–20193.
41. Park, H., Suquet, C., Satterlee, J. D., and Kang, C. (2004) Insights into signal transduction involving PAS domain oxygen-sensing heme proteins from the X-ray crystal structure of *Escherichia coli* Dos heme domain (Ec DosH). *Biochemistry 43*, 2738–2746.
42. Scott, C., Guest, J. R., and Green, J. (2000) Characterization of the *Lactococcus lactis* transcription factor FlpA and demonstration of an in vitro switch. *Mol. Microbiol. 35*, 1383–1393.
43. Gostik, D. O., Green, J., Irvine, A. S., Gasson, M. J., and Guest, J. R. (1998) A novel regulatory switch mediated by the FNR-like protein of *Lactobacillus casei*. *Microbiology 144*, 705–717.
44. Yanish-Perron, C., Vieira, J., and Messing, J. (1985) Improved M13 phage cloning vectors and host strains: Nucleotide sequence of the M13mp18 and pUC19 vectors. *Gene 33*, 103–119.
45. Savitzky, A., and Golay, M. J. E. (1964) Smoothing and Differentiation of Data by Simplified Least Square Procedures. *Anal. Chem. 36*, 1627–1639.
46. Rost, B., Yachdav, G., and Liu, J. (2004) The PredictProtein Server. *Nucleic Acids Res. 3*, 321–326.
47. Larkin, M. A., Blackshields, G., Brown, N. P., Chenna, R., McGettigan, P. A., McWilliam, H., Valentin, F., Wallace, I. M., Wilm, A., Lopez, R., Thompson, J. D., Gibson, T. J., and Higgins, D. G. (2007) ClustalW2 and ClustalX version 2. *Bioinformatics 23*, 2947–2948.
48. Saitou, N., and Nei, M. (1987) The neighbor-joining method: A new method for reconstructing phylogenetic trees. *Mol. Biol. Evol. 4*, 406–425.

BI8014086